Available online at www.sciencedirect.com
SCIENCE DIRECT®
C. R. Physique 6 (2005) 313–320
COMPTES RENDUS PHYSIQUE
http://france.elsevier.com/direct/COMREN/

The Near Earth Objects: possible impactors of the Earth/Les astéroïdes geocroiseurs : impacteurs potentiels de la Terre

NEO sizes, shapes and surface physical properties

A. Chantal Levasseur-Regourd [a,*], Marcello Fulchignoni [b], Marco Delbó [c], Richard P. Binzel [d]

[a] *Université P. et M. Curie, Aéronomie CNRS-IPSL, BP 3, 91371 Verrières, France*
[b] *LESIA, Observatoire de Paris, 5, place J. Janssen, 92195 Meudon Principal cedex, France*
[c] *INAF, Osservatorio Astronomico di Torino, via Osservatorio 20, 10025 Pino Torinese, Italy*
[d] *MIT-EAPS, 77, Massachusetts avenue, Cambridge, MA 02139, USA*

Available online 25 February 2005

Presented by Pierre Encrenaz

Abstract

The sizes, shapes, and surface or subsurface properties of Near Earth Objects (mostly asteroids, also inactive comet nuclei) are still poorly known, since any accurate determination requires in situ missions. It may nevertheless be estimated that the sizes of these irregular bodies range from a few tens of kilometres to a few tens of meters, with possibly about 1000 NEOs with sizes greater than 1 km. Their surfaces are estimated to be quite rough, and at least partially covered with regolith. ***To cite this article: A.C. Levasseur-Regourd et al., C. R. Physique 6 (2005).***

Résumé

Les tailles, formes et propriétés de surface ou sous surface des géocroiseurs sont encore mal connues, dans la mesure où leur détermination repose sur l'exploration locale. Ces objets irréguliers (essentiellement des astéroïdes, mais aussi des noyaux cométaires inactifs) ont des tailles allant de quelques kilomètres à quelques mètres, avec environ un millier d'entre eux dépassant le kilomètre. Les surfaces semblent assez rugueuses et sont couvertes, au moins partiellement, de régolites. ***Pour citer cet article : A.C. Levasseur-Regourd et al., C. R. Physique 6 (2005).***

Keywords: Asteroids; Comets; NEOs; Size; Shape; Surface physical properties

Mots-clés : Astéroïdes ; Comètes ; Géocroiseurs ; Taille ; Forme ; Propriétés physiques de surface

1. Introduction

A better knowledge of the physical properties of Near Earth Objects (thereafter NEOs) is mandatory to estimate the risks of an impact and optimize survey strategies. More specifically, the determination of surface and subsurface properties (i.e. porosity, size of the irregularities) is required to define the efficiency of penetrators and anchoring devices; it would be vital for any attempt to mitigate the risks of a potentially hazardous object.

* Corresponding author.
E-mail address: Chantal.Levasseur@aerov.jussieu.fr (A.C. Levasseur-Regourd).

1631-0705/$ – see front matter
doi:10.1016/j.crhy.2005.01.003

Information on the shapes, albedo, and size distribution of NEOs is also mandatory for any attempt to investigate their physical nature, mineralogy, taxonomy and origins, and to understand the physical processes that played a role in their evolution.

The NEO population actually consists of asteroids (or fragments thereof), i.e. mostly rocky objects; it also consists of cometary nuclei, i.e. icy objects and small inactive nuclei (so-called defunct or dormant comets), which have lost all their ices or are coated by an insulating dust mantle. Asteroids most likely represent the main population. However, inactive and active comets could represent about up to 18% and 1%, respectively, of the total population [1]. It is thus necessary to consider the physical properties of both asteroids and comets, specially taking into account the fact that cometary orbits may be quite elongated and inclined with respect to the Earth orbital plane, leading to high relative velocities and impact energies.

NEOs parent bodies have been formed over a large range of solar distances in the early solar system, with different temperatures, compositions and concentrations; moreover, they have been going through various evolution processes, in relation to their collision and evaporation history. NEOs thus exhibit a wide diversity in their properties. After describing our present knowledge about their sizes, shapes and surface morphology, we will analyze their surface properties, as derived from thermal and light scattering observations.

2. Sizes, shape and craterisation of near-Earth asteroids

2.1. Direct observations

The precise shape of a NEO is known only in the case of asteroid 433 Eros (Fig. 1(left)), the target of the one-year long orbital NEAR-Shoemaker mission. The images show that it is elongated, with a shape roughly fitted by a McLaurin ellipsoid of 34.4 km $\times$ 11.2 km $\times$ 11.2 km axis. The surface seems to be mostly covered by a regolith, i.e. a layer of fragmentary incoherent rocky debris, which nearly everywhere forms the surface terrain. Of special interest is the evidence for down-slope motion and flat ponds of smaller debris inside some craters of a few tens of meters [2].

Information on cratering records on asteroid surfaces has been obtained from Galileo images of 951 Gaspra, 243 Ida (and its moon Dactyl) and from NEAR-Shoemaker images of 253 Mathilde and 433 Eros. From this limited sample, the cratering history of NEOs does not seem to differ significantly from that of main belt objects. Crater populations (size above 100 m) on Ida and Eros are similar and show very high crater densities. Gaspra has a few large craters but has been riddled with a large number of small and 'fresh' craters. Mathilde is dominated by huge craters, with diameters close to its radius. Such differences amongst these bodies have been attributed to differences in the bulk structure of the asteroids [3].

Fig. 1. Left: Asteroid Eros, from a mosaic of images obtained in December 2000. The saddle-shape feature Himeros is visible just above the centre of the image, together with impact craters and local heterogeneities in the surface texture (NASA, NEAR-Shoemaker). Right: Nucleus of comet Wild 2, as imaged in January 2004. Surface depressions, some of which could be impact craters, pinnacles and albedo features may be noticed on the surface (Nasa, Stardust, see also [16,17]).

2.2. Remote observations

Remote observations provide most of the available estimates on asteroid shapes. The applied techniques are: (i) lightcurve inversion method with or without additional information from synthetic lightcurves obtained from laboratory simulation or numerical models [4]; (ii) sophisticated modelling from a very large set of disk integrated data [5]; and (iii) radar observations [6]. The accuracy of each method depends on the completeness of the data sets and on the observation technique.

Broad-band photometry (mostly in V and R bands) is the main source of lightcurve data. Barucci et al. [7] suggested the use Fourier analyses of asteroids lightcurves with substantially complete phase coverage and point density and the use of synthetic lightcurves from models different in shape, orientation and albedo markings, in order to possibly derive the shape and albedo variations by comparing model and asteroid lightcurve coefficients. If a small set of high quality lightcurves obtained at different ecliptic longitudes is available, it is possible to deduce both the asteroid pole direction and the a/b and b/c ratio between the axes of the ellipsoid fitting the real shape of the asteroid [8]. The various methods based on the above techniques have been used to recover the shape of Gaspra, the first asteroid target of a spacecraft mission [4]. The comparison between the real shape of Gaspra, obtained from Galileo, and the results of the lightcurves analysis shows that the bulk shape can be obtained with a relatively small amount of data (three to five lightcurves).

If several lightcurves obtained at various geometries are available, the resulting convex inversion is unique and stable and provides the rotation period, pole direction, and scattering parameters simultaneously with the shape. The recovered shapes are general and not based on modifications of any prior shape model. Kaasalainen et al. [9] present shape, pole, and period solutions for asteroids that have also been observed by space probes or radar.

Radar is a powerful source of information about the physical properties and orbits of asteroids. Measurements of the distribution of echo power in time delay (range) and Doppler frequency (radial velocity) produce two-dimensional images with a resolution of up to few meters, in the case of very high signal-to-noise echo returns. These images can be used to construct detailed three-dimensional models if a wide coverage in orientation is obtained. In most cases, radar is the only ground-based technique that spatially resolves near-Earth objects. Ostro et al. [6] have summarized the results for 105 near-Earth asteroids, which span four orders of magnitude in diameter and rotation period. Radar has shown the great variety of near-Earth objects: spheroids and highly elongated shapes, contact-binary shapes, and binary systems. More and more NEOs have indeed been discovered to be binary systems, with forty six couples known while this paper is written [11] and 16% of NEOs larger than 200 meters estimated to be binary systems [12]. Radar experiments also provide an estimation of the near surface porosity. For 433 Eros, this approach leads to a surface porosity of about 47% [10].

Finally, the known NEO population includes thousands of objects ranging from ten or so kilometers to ten or so meters. The data obtained with the above-described methods show that generally these objects have elongated irregular shapes. Satellite sizes are in the range of 0.2 to 0.5 of the primary's diameter. Secondary rotations appear mostly (but not generally) synchronized with the mutual orbital motions. While primaries show lightcurves with low amplitudes indicating that they have roughly spheroidal shapes with low equatorial elongations, secondary lightcurves suggest that some of them have more elongated shapes [13].

3. Size, shape and surface morphology of cometary nuclei

Comet nuclei gravitate on rather elongated orbits around the Sun, and eject gases and dust when the solar radiation is sufficient enough to allow some evaporation of their ices. They are either point sources when they are far from the Sun (and the Earth), or are hidden by their bright coma when they get closer to the Sun. Detection of near-Earth inactive nuclei is also difficult, since they are likely to be small and dark objects. Precise determination of their size, shape and morphology is thus only possible through in-situ missions, although some indirect information may also be obtained.

3.1. Direct observations

Only three comet nuclei have up to now been imaged: 1P/Halley, 19P/Borelly and 81P/Wild 2, respectively by Giotto in 1986, Deep Space 1 in 2001 and Stardust in 2004. The sizes and shapes approximately correspond to ellipsoids with axis diameters of respectively $15.3 \times 7.2 \times 7.2$ km [14], 8.0 km $\times$ 3.2 km $\times$ 3.2 km [15] and 5.5 km $\times$ 4.0 km $\times$ 3.3 km [16]. A comparison of the images immediately reveals a significant diversity in overall shapes and topographic features. The nucleus of Wild 2 (Fig. 1(right)), much more round than the nuclei of Halley and Borelly, is littered with depressions, and a large variety of landforms (including areas likely to consist of porous cohesive material) are observed. Some cometary nuclei are likely to be gravitational aggregates of smaller bodies (so-called rubble-piles), while others could be more compact [17].

3.2. Remote observations

It is possible, from high-resolution remote observations (with e.g. HST), to separate the signal of the nucleus from that of the coma, and to derive its mean radius (with an assumption on the albedo and on the phase dependence of the magnitude). Moreover, the lightcurve allows the derivation of the rotational period and of the a/b ratio of the assumed ellipsoidal nucleus. Lamy et al. [18] have successfully predicted values of a and b equal to 8.8 km and 3.6 km, respectively, for Borelly.

Other indirect approaches may be used, such as radar observations and simultaneous thermal and optical observations. From two different approaches, the nucleus of the remarkably bright and active comet C/1995 01 Hale-Bopp has been estimated to be in a 56 km to 30 km size range [19,20].

Based on data obtained with HST and Keck telescopes, Meech et al. [21] suggest that the size distribution correspond to a ($r^{-3.5}$) collisional population law, truncated for radii below about 2 km. Small nuclei are actually expected to disappear, because of outgassing, complete disruption and partial fragmentation. Fragmentation processes are quite usual. The presence of multiple icy fragments with sizes up to a hundred meters had been inferred from observations of C/1996 B2 Hyakutake [22]. It is also most likely that the huge cloud of dust particles encountered by Stardust resulted from the progressive disintegration of a fragment of Wild 2, of the order of one meter across [23,24]. The surface layer of most nuclei might actually easily 'crumble' in meter or sub-meter sized fragments.

4. Size and albedo, as derived from thermal observations

Measurements of the thermal continua of asteroids (longwards of 5 μm, but from the ground limited by the atmospheric absorption to 20 μm), combined with simultaneous visible magnitudes and a suitable model of the surface thermal emission (thermal model) is a powerful technique to derive sizes and albedos of asteroids. Observations carried out by IRAS satellite [25] have provided size and albedo information for more than 2000 main-belt asteroids, representing a major milestone in the physical characterization of minor planets. However, this is not the case for the NEO population. NEOs are small and faint targets, the infrared observations of which are a challenge requiring the largest telescopes in the world.

4.1. NEO size distribution from infrared observations

The physical characterization of NEOs from thermal infrared observations is a promising technique that has up to now provided the large majority of their sizes and albedos [26–28]. Recent long-term observational programs have incremented the number of NEOs with measured sizes and albedos by 54% [28,29]. The bias-corrected NEO population has been modelled by combining this database of albedos with the largest dataset of NEOs taxonomies [1,30], leading to a bias-corrected mean albedo for the NEO population of 0.14 ± 0.02, for which an (H) magnitude of 17.8 ± 0.1 translates to a diameter of 1 km, in close agreement with the Morbidelli et al. [31] model. On the basis of the taxonomic and albedo corrected NEO population model, the H-magnitude has been translated to a diameter distribution, with 1090 ± 180 NEOs with diameter larger than 1 km. However, albedo measurements are available for only about 4% of the total NEO population, and the large contribution from the X-types strongly suggests the need to better characterize this group with more albedo measurements.

4.2. Thermal inertia of NEOs from infrared observations

The application of thermal infrared techniques to NEOs presents special problems due to the wide range of solar phase angles at which they are observed and the fact that, compared to observed main-belt asteroids, NEOs are small and irregular (e.g. [32,33]). Several authors (e.g. [26,34–36]) have explained inconsistencies found between radiometric albedos and albedos derived by radar or inferred from taxonomic classification, by the lack of a significant insulating layer of regolith on some NEO surfaces. It implies a thermal inertia higher with respect to that of the main belt asteroids.

Thermal inertia, which represents quantitatively the resistance of a material to temperature changes during a full heating/cooling cycle, can be used to estimate the average grain size of a particulate surface material [37]. Lower values are indicative of loose, fine-grained sediments that loose heat rapidly. Increasingly consolidated sediments and coarser-grained materials (i.e., sand, gravel, boulders, and bedrock) have higher heat retention and therefore they produce progressively higher thermal inertia values. Recent studies [28], using a near-Earth asteroid thermal model [27] to derive radiometric diameters and albedos, put constraints on how high the NEOs thermal inertia can be. In this model, the η-parameter describes numerically how the observed surface temperature distribution deviates from that of a smooth surface with no thermal inertia in thermal equilibrium with solar insolation ($\eta = 1.0$ for every value of the phase angle). Fig. 2 shows that the large majority of NEOs have rather low η-values scattered around a straight line. A detailed analysis [28] provides growing evidence to the fact that NEOs thermal inertia is usually much lower than that of exposed bare rock. Such values imply surfaces at least partially covered with regolith.

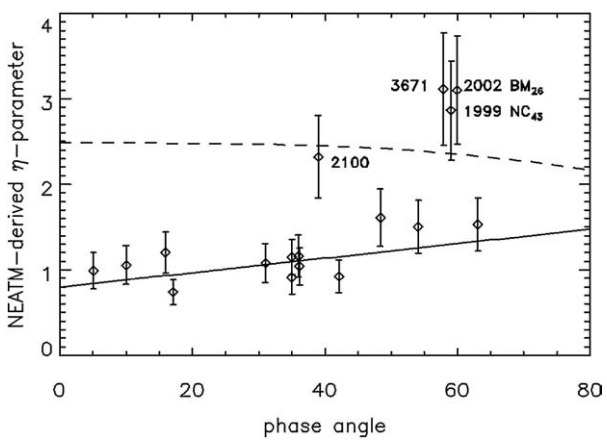

Fig. 2. Best-fit η parameter, as derived by the near-earth asteroid thermal model, against phase angle α. The continuous straight-line represents a linear fit, $\eta = (0.008 \pm 0.002)\alpha + (0.81 \pm 0.07)$ to all values of $\eta < 2$. Diamonds at $\eta > 2$ are data points considered anomalous. The dashed curve represents the expected η values for an asteroid with a thermal inertia consistent a surface of exposed bare rocks. The large majority of η-values are scattered around 1.25 and much below the dashed curve. It is argued that this is an indication of surfaces with moderate values of thermal inertia (from [28]).

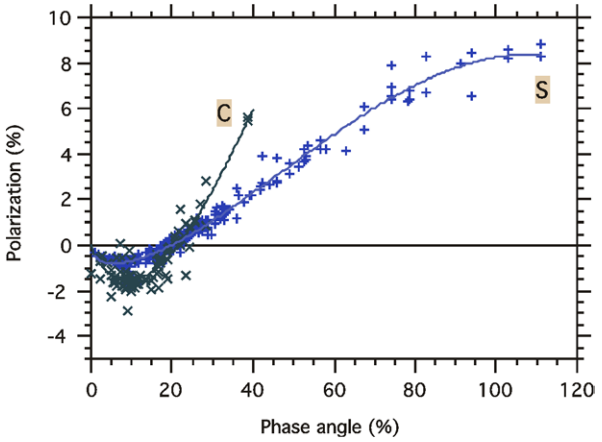

Fig. 3. Observed dependence of the polarization of asteroid surfaces upon the phase angle for (+) bright S-types and (×) dark C-types. The trends are typical of scattering by irregular particles with sizes greater than the wavelength.

5. Texture, as derived from asteroids light scattering observations

Light scattering gives unique clues about the texture of the regolithic surface (see e.g. [38,39]). Solar light scattered by such irregular surfaces is partially linearly polarized. While the intensity (Z) scattered in a given direction is the sum of two polarized components (with the electric field vector respectively parallel and perpendicular to the scattering plane), the linear polarization P is defined by the ratio of the difference to the sum of these two components (see e.g. [40]):

$$Z = (Z_\perp + Z_\parallel), \qquad P = (Z_\perp - Z_\parallel)/(Z_\perp + Z_\parallel).$$

The polarization only varies with the solar phase angle α, with the wavelength λ, and with the physical properties of the surface. Polarization can thus be used to compare data obtained at different times, on different regions and on different objects.

5.1. Phase angle and wavelength dependence of the polarization

The changing geometry of a NEO and of the observer with respect to the Sun is used to define a (disk integrated) polarization phase curve, tentatively between 0° (backscattering) and 180° (forward scattering). Asteroidal polarization phase curves are similar to those of numerous particulate media in the solar system, such as the Moon or cometary dust (see e.g. [38,41]). As illustrated in Fig. 3, they are smooth, with a small negative branch near backscattering (where $Z_\parallel$ predominates over $Z_\perp$), an inversion region near 20°, followed by a wide positive branch with a near 90° maximum. Such curves have been estimated by various authors to be typical of the interaction of light with irregular particles media, with a size larger than the wavelength.

A sharp increase of the negative polarization may be noticed near backscattering (together with a non linear enhancement of the intensity towards smaller phase angles). It is attributed to optical effects within a porous regolitic surface, i.e. mutual shadowing and coherent backscattering.

Different slopes at inversion (or different maxima in polarization for NEOs observed at large phase angles) are easily noticed in Fig. 3. The slope at inversion (as well as the value of the maximum) usually increases with decreasing values of the albedo (A). Taking into account the fact that (Z) is proportional to (A), this relationship, so-called Umov law, indicates that the correlation between $(Z_\perp - Z_\parallel)$ and (A) is very weak [42]. It is actually related to the surface roughness and to the existence of multiple scattering in the subsurface. The slope at inversion can thus be used to derive from clustering analysis a classification similar to asteroidal taxonomy, with two main classes corresponding respectively to bright (S, M and E types) asteroids and dark (C, G and P types) asteroids (see e.g. [43,44]).

The numerous observations performed by different teams on 4179 Toutatis (e.g. [45]), a S-type object, indicate [39] that: (i) the phase curves obtained in different colours have almost the same inversion point (near 20°); (ii) the maximum is reached near 100°; (iii) the polarization decreases linearly with increasing wavelength in the 20° to 90° phase angles range, the decrease getting steeper from 20° to 90°.

Observations of 2100 Ra-Shalom, a C-type object [46] lead to a similar inversion angle, but the polarization hardly varies with the wavelength. This discrepancy suggests that the surface physical properties are different, not only in terms of albedo, but also in terms of size distribution of the irregularities.

To summarize, NEOs surfaces are likely to be covered by porous and rough regolitic layers. However, they are certainly far from being homogeneous, and the presence of harder consolidated areas cannot be ruled out, as emphasized by the detection of local variations in the physical characteristics. Some parameters in the light scattering properties (e.g. maximum in polarization phase curve, polarization wavelength dependence) differ significantly from one object to the next. They need to be exactly translated in terms of morphological properties of the particulate media building up the surfaces.

5.2. Interpretation through simulations of light scattering observations

The light scattering properties of fractal aggregates of spheroidal (mono-disperse or core-mantle) monomers can be computed through Discrete Dipole Approximation codes, for various size parameters and complex refractive indices. The negative branch of polarization at small phase angles appears as soon as the size of the aggregate is of the order of the wavelength. Also, a comparison between the phase curves obtained for aggregates with the same amount of identical monomers, suggests that porous aggregates are likely to correspond to a higher polarization than more compact aggregates.

Monte-Carlo techniques have been recently developed by Muinonen [47] to take into account the multiple scattering, with both coherent backscattering and radiative transfer theories, for semi-infinite plane-parallel media of spherical monodisperse scatterers with various size parameters. They are being compared with laboratory measurements on highly porous 'cakes' of silica spheres [48].

Experimental simulations indeed provide a complementary approach, since they avoid computations of multiple scattering by irregular particles, as well as various assumptions (value of the complex refractive indices, morphology of the medium, surface irregularities). The obtained polarization phase curves are reminiscent of the observed ones and demonstrate that the maximum in polarization depends upon the size, the albedo and the porosity of the scattering medium.

Fig. 4 presents recent results obtained on various samples in the laboratory with the PROGRA^2 instrument (see e.g. [49]), with sifted particles, the porosity of which should be quite representative of that of asteroidal regoliths. The maximum in polarization increases with the average size of compact particles, up to a level that depends upon the refracted light absorption, i.e. upon the characteristics of the sample. It also decreases with the albedo, the decrease being stronger for porous layers. Simultaneous determination of the thermal and light scattering properties of a given region of a NEO would indeed allow a decent determination of its albedo, size distribution and porosity.

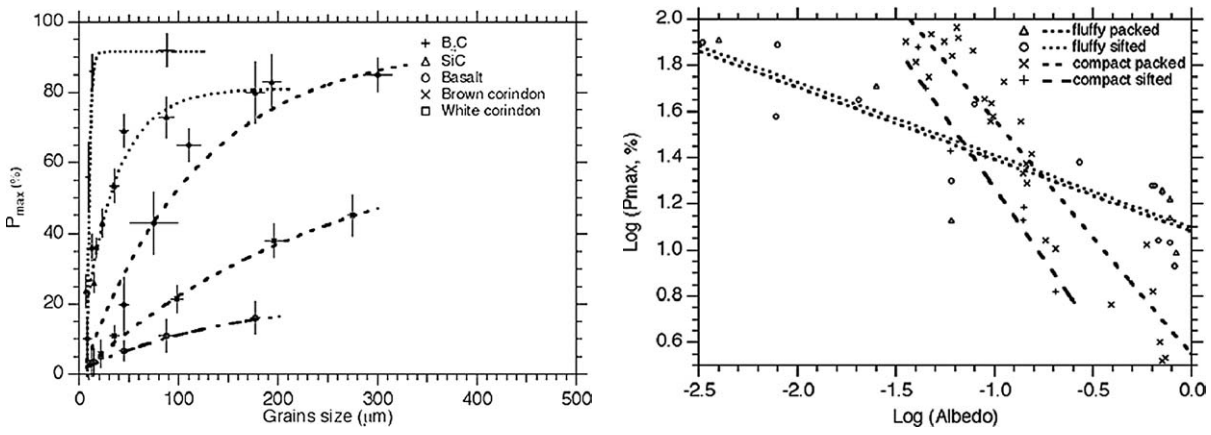

Fig. 4. Dependence of the maximum in polarization (as deduced from experimental simulations) upon: (a) the size of the scattering grains and (b) the albedo. For a given material, lower values may be a clue to a lower size of the compact grains building up the regolith, and/or to a higher porosity of the regolith.

6. Perspectives

NEOs are small irregular bodies (mostly asteroids, also inactive comets nuclei and fragments thereof), whose shapes and surface morphologies are still poorly known. Space missions represent an invaluable source of information, to be used as a 'ground truth' in interpreting remote observations. They have provided and will continue to provide us with most of the required information. New precious observations of the big asteroid 21 Lutetia and the small asteroid 2867 Steins, as well as of the nuclei of comets 67P/Churyumov–Gerasimenko and 9P/Tempel 1, are expected from Rosetta and Deep Impact space missions in the coming years.

Meanwhile, more remote observations, on a large range of wavelengths (from the optical to the thermal infrared ranges), over a wide range of phase angles, with possibly retrieval of the whole Mueller matrix of the scattered light, are expected. Significant refinements of the thermal models will be possible thanks to SIRTF observations of small asteroids from Earth orbit. Light scattering models will benefit from the results coming from laboratory simulations under microgravity conditions. These improvements will allow us to obtain a more precise determination of the key parameters, which describe the physical characteristics of the NEOs.

Acknowledgements

Support from ESA, CNES and French PNP is acknowledged.

References

[1] R.P. Binzel, A.S. Rivkin, J.S. Stuart, A.W. Harris, S.J. Bus, T.H. Burbine, Observed spectral properties of near-Earth objects: results for population distribution, source regions, and space weathering processes, Icarus 170 (2004) 259–294.
[2] P.C. Thomas, J. Joseph, B. Carcich, J. Veverka, B.E. Clark, J.F. Bell III, A.W. Byrd, R. Chomko, M. Robinson, S. Murchie, L. Prockter, A. Chen, N. Izenberg, M. Malin, C. Chapman, L.A. McFadden, R. Kirk, M. Gaffey, P.G. Lucey, Eros: shape, topography, and slope processes, Icarus 155 (2002) 18–37.
[3] C.R. Chapman, Cratering on asteroids from Galileo and NEAR-Shoemaker, in: W.F. Bottke Jr., A. Cellino, P. Paolicchi, R.P. Binzel (Eds.), Asteroids III, University of Arizona Press, Tucson, 2002, pp. 315–330.
[4] M.A. Barucci, A. Cellino, C. de Sanctis, M. Fulchignoni, K. Lumme, V. Zappala, P. Magnusson, Ground-based Gaspra modelling – comparison with the first Galileo image, Astron. Astrophys. 266 (1992) 385–394.
[5] M. Kaasalainen, S. Mottola, M. Fulchignoni, Asteroid models from disk-integrated data, in: W.F. Bottke Jr., A. Cellino, P. Paolicchi, R.P. Binzel (Eds.), Asteroids III, University of Arizona Press, Tucson, 2002, pp. 139–150.
[6] S.J. Ostro, R.S. Hudson, L.A.M. Benner, J.D. Giorgini, C. Hagri, J.L. Margot, M.C. Nolan, Asteroid Radar Astronomy, in: W.F. Bottke Jr., A. Cellino, P. Paolicchi, R.P. Binzel (Eds.), Asteroids III, University of Arizona Press, Tucson, 2002, pp. 151–168.
[7] M.A. Barucci, M.T. Capria, A.W. Harris, M. Fulchignoni, On the shape and albedo variegation of asteroids – results from Fourier analysis of synthetic and observed asteroid lightcurves, Icarus 78 (1999) 311–322.
[8] P. Magnusson, M.A. Barucci, J.D. Drummond, K. Lumme, S.J. Ostro, Determination of pole orientations and shapes of asteroids, in: R.P. Binzel, T. Gehrels, M.S. Matthews (Eds.), Asteroids II, University of Arizona Press, Tucson, 1989, pp. 67–97.
[9] M. Kaasalainen, J. Torppa, K. Muinonen, Optimization methods for asteroid lightcurve Inversion. II. The complete inverse problem, Icarus 153 (2001) 37–51.
[10] C. Magri, G.J. Consolmagno, S.J. Ostro, L.A. Benner, B.R. Beeney, Radar constraints on asteroid regoliths properties using 433 Eros as ground truth, Meteor. Planet. Sci. 36 (2001) 1697–1709.
[11] W.R. Johnstone, http://www.johnstonsarchive.net/astro/asteroidmoons.html, 2004.
[12] J.L. Margot, M.C. Nolan, L.A.M. Benner, S.J. Ostro, R.F. Jurgens, J.D. Giorgini, M.A. Slade, D.B. Campbell, Binary asteroids in the Near-Earth Objects population, Science 296 (2002) 1445–1448.
[13] P. Pravec, et al., Photometric Survey of Binary Near-Earth Asteroids, Bull. Am. Astron. Soc. 36 (2004) 1131.
[14] H.U. Keller, W.A. Delamere, H.J. Reitsema, W.F. Huebner, H.U. Schmidt, Comet P/Halley's nucleus and activity, Astron. Astrophys. 187 (1987) 807–823.
[15] L.A. Soderblom, T.L. Becker, G. Bennett, D.C. Boice, D.T. Britt, R.H. Brown, B.J. Burratti, C. Isbell, Observations of comet, 19P/Borrelly by the miniature integrated camera aboard Deep Space 1, Science 296 (2002) 1087–1091.
[16] D.E. Brownlee, F. Horz, R.L. Newburn, M. Zolensky, T.C. Duxbury, S. Sandford, Z. Sekanina, P. Tsou, M.S. Hanner, B.C. Clark, S.F. Green, J. Kissel, Surface of young Jupiter family comet 81P/Wild 2, Science 304 (2004) 1764–1769.
[17] H.A. Weaver, Not a rubble pile?, Science 304 (2004) 1760–1762.
[18] P. Lamy, I. Toth, H.A. Weaver, Hubble Space Telescope observations of the nucleus and inner coma of comet 19P/1904 Y2 (Borrelly), Astron. Astrophys. 337 (1998) 945–954.
[19] L. Jorda, P. Lamy, O. Groussin, I. Toth, M.F. A'Hearn, S. Peschke, ISOCAM observations of cometary nuclei, ESA SP-455 (2000) 61–66.
[20] Y.R. Fernandez, The nucleus of comet Hale-Bopp (C/1995 01): size and activity, Earth, Moon, Planets 89 (2002) 3–25.

[21] K.J. Meech, O.R. Hainaut, B.G. Marsden, Comet nucleus size distribution from HST and Keck telescopes, Icarus 170 (2004) 463–491.
[22] E. Desvoivres, J. Klinger, A.C. Levasseur-Regourd, Modelling the dynamics of fragments of cometary nuclei: application to comet C/1996 B2 Hyakutake, Icarus 144 (2000) 172–181.
[23] Z. Sekanina, D.E. Brownlee, T. Economou, A.J. Tuzzolino, S.F. Green, Modelling the nucleus and jets of comets 81P/Wild 2 on the Stardust encounter data, Science 304 (2004) 1769–1774.
[24] A.C. Levasseur-Regourd, Cometary dust unveiled, Science 304 (2004) 1762–1763.
[25] E.F. Tedesco (Ed.), The IRAS Minor Planet Survey. Tech. Rep. PLTR-92-2049. Phillips Laboratory, Hanscom Air Force Base, MA, 1992.
[26] G.J. Veeder, M.S. Hanner, D.L. Matson, E.F. Tedesco, L.A. Lebofsky, A.T. Tokunaga, Radiometry of near-Earth asteroids, Astron. J. 97 (1989) 1211–1219.
[27] A.W. Harris, A thermal model for near-Earth asteroids, Icarus 131 (1998) 291–301.
[28] M. Delbó, A.W. Harris, R.P. Binzel, P. Pravec, J. Davies, Keck observations of near-Earth asteroids in the thermal infrared, Icarus 166 (2003) 116–130.
[29] M. Delbó, The nature of near-Earth asteroids from the study of their thermal infrared emission, Ph.D. thesis Freie Universität Berlin, June 2004.
[30] J.S. Stuart, R.P. Binzel, Bias-corrected population, size distribution, and impact hazard for the near-Earth objects, Icarus 170 (2004) 295–311.
[31] A. Morbidelli, R. Jedicke, W.F. Bottke, P. Michel, E.F. Tedesco, From magnitudes to diameters: the albedo distribution of near Earth objects and the Earth collision hazard, Icarus 158 (2002) 329–342.
[32] A.W. Harris, J.S.V. Lagerros, Asteroids in the thermal infrared, in: W.F. Bottke Jr., A. Cellino, P. Paolicchi, R.P. Binzel (Eds.), Asteroids III, University of Arizona Press, Tucson, 2002, pp. 205–218.
[33] M. Delbó, A.W. Harris, Physical properties of near-Earth asteroids from thermal infrared observations and thermal modelling, Meteorit. Planet. Sci. 37 (2002) 1929–1936.
[34] D. Morrison, The diameter and thermal inertia of 433 Eros, Icarus 28 (1976) 125–132.
[35] A.W. Harris, J.K. Davies, S.F. Green, Thermal infrared spectrophotometry of the near-Earth Asteroids 2100 Ra-Shalom and 1991 EE, Icarus 135 (1998) 441–450.
[36] A.W. Harris, J.K. Davies, Physical characteristics of near-Earth asteroids from thermal infrared spectrophotometry, Icarus 142 (1999) 464–475.
[37] L.K. Fenton, R.L. Fergason, Thermal properties of sand from TES and THEMIS: Do Martian dunes make a good control for thermal inertia calculations?, in: 35th Lunar and Planetary Science Conference, 2004. Online version at http://www.lpi.usra.edu/meetings/lpsc2004/pdf/1974.pdf.
[38] K. Muinonen, J. Piironen, Y.G. Shkuratov, A. Ovcharenko, B.E. Clark, Asteroid photometric and polarimetric phase effects, in: W.F. Bottke Jr., A. Cellino, P. Paolicchi, R.P. Binzel (Eds.), Asteroids III, University of Arizona Press, Tucson, 2002, pp. 123–138.
[39] A.C. Levasseur-Regourd, Polarimetry of dust in the solar system: remote observations, in-situ measurements and experimental simulations, in: G. Videen, Y. Yatskiv, M. Mishchenko (Eds.), Photopolarimetry in Remote Sensing, NATO Series, Kluwer Academic, Dordrecht, 2004, pp. 393–410.
[40] B. Hapke, Theory of Reflectance and Emittance Spectroscopy, Cambridge University Press, Cambridge, 1993.
[41] A.C. Levasseur-Regourd, E. Hadamcik, Light scattering by irregular dust particles in the solar system: observations and interpretation by laboratory measurements, J. Quant. Spectros. Radiat. Transfer 79 (2003) 903–910.
[42] V.G. Shkuratov, N.V. Opanasenko, Polarimetric and photometric properties of the Moon: telescope observation and laboratory simulation, Icarus 99 (1992) 468–484.
[43] B. Goidet-Devel, J.B. Renard, A.C. Levasseur-Regourd, Polarization of asteroids: Synthetic curves and characteristic parameters, Planet. Space Sci. 43 (1995) 779–786.
[44] A. Pentillä, K. Lumme, E. Hadamcik, A.C. Levasseur-Regourd, Statistical analysis of asteroidal et cometary phase curves, Astron. Astrophys., 2004, in press.
[45] M. Ishiguro, H. Nakayama, M. Kogachi, T. Mukai, R. Nakamura, R. Hirata, A. Okazaki, Maximum visible polarization of 4179 Toutatis in the apparition of 1996, Publ. Astron. Soc. Japan 49 (1997) L31–L34.
[46] N.N. Kiselev, V.K. Rosenbush, K. Jockers, Polarimetry of asteroid 2100 Ra-Shalom at large phase angle, Icarus 140 (1999) 464–466.
[47] K. Muinonen, Coherent backscattering of light by complex random media of spherical scatterers: numerical solution, Waves Random Media 14 (2004) 365–388.
[48] E. Hadamcik, J.B. Renard, A.C. Levasseur-Regourd, J.C. Worms, PROGRA^2 experiment: new results for dust clouds and regoliths analogs, Adv. Space Res., 2004, submitted for publication.
[49] J.C. Worms, J.B. Renard, E. Hadamcik, A.C. Levasseur-Regourd, J.F. Gayet, Results of the PROGRA^2 experiment: an experimental study in microgravity of scattered polarised light by dust particles with large size parameter, Icarus 142 (1999) 281–297.